

Anisotropic manifestation of short-range magnetic correlations in $\text{Ce}_{0.6}\text{La}_{0.4}\text{RhIn}_5$ V. F. Correa,¹ L. Tung,¹ S. M. Hollen,² P. G. Pagliuso,¹ N. O. Moreno,¹ J. C. Lashley,¹ J. L. Sarrao,¹ and A. H. Lacerda¹¹*Los Alamos National Laboratory, Los Alamos, New Mexico 87545, USA*²*Occidental College, Los Angeles, California 90041, USA*

(Received 9 February 2004; published 25 May 2004)

We report thermal-expansion and magnetostriction results on $\text{Ce}_{0.6}\text{La}_{0.4}\text{RhIn}_5$ single crystals. This particular La concentration ($x_c \sim 0.4$) corresponds to the critical one at which the long-range magnetic order vanishes ($T_N=0$). However, as also observed in specific heat and magnetic susceptibility measurements, a large “hump” is seen in thermal-expansion at $T_{\text{SR}} \sim 4.5$ K. This anomaly, claimed to be related to short-range correlations, is observed only along the c axis, confirming that anisotropy plays an important role in these 115 compounds. No particular feature is associated with the magnetic correlations in the magnetostriction measurements. The magnetic field dependence of the volume is quadratic in field as expected for a paramagnetic system, above and below T_{SR} . Finally, the magnetic field dependence of the crystal electric field contribution to the thermal expansion seems to reinforce the idea that the La doping leads to a $|\pm 5/2\rangle$ -rich ground state doublet.

DOI: 10.1103/PhysRevB.69.174424

PACS number(s): 75.80.+q, 75.40.-s, 71.27.+a, 65.40.De

I. INTRODUCTION

The physics of heavy fermions (HF's) is dominated by the competition between different microscopic mechanisms (and related energy scales) and this results in a wide spectrum of different ground states including unconventional superconductivity and magnetic order.¹ The magnetic properties (resulting from the interaction between the f -localized magnetic moments and the free electron spins) are determined by the competition between the long range Ruderman-Kittel-Kasuya-Yosida (RKKY) interaction and the short range Kondo effect, both of which depend on the magnetic exchange parameter J . This gives rise to magnetic order or a nonmagnetic Kondo singlet state, respectively. Moreover, changing macroscopic variables such as pressure, magnetic field, or doping can lead to significant changes in the microscopic parameter J producing new ground states.²

These features are exemplified in the recently discovered CeMIn_5 ($M = \text{Co}, \text{Rh}, \text{Ir}$) family.³⁻⁵ These compounds crystallize in the tetragonal HoCoGa_5 -like structure consisting of alternating layers of magnetic CeIn_3 and nonmagnetic $M\text{In}_2$ along the c axis. Long-range antiferromagnetism as well as hybridization and mass enhancement due to the Kondo effect have been observed in the 115 family.³ Also, magnetically mediated superconductivity and non-Fermi-liquid (NFL) behavior have been reported.^{3,5-7}

In particular, CeRhIn_5 shows ambient pressure antiferromagnetism³ ($T_N = 3.8$ K) and pressure induced superconductivity^{3,8} ($T_c = 2.1$ K at $P = 16$ kbar). Neutron diffraction experiments⁹ reveal a reduced magnetic moment associated with the Ce ions ($0.75\mu_B$ compared to $0.92\mu_B$ expected for the ground state doublet) suggesting an important Kondo compensation. This is corroborated by specific heat measurements³ that show only 30% of $R \ln 2$ entropy released up to T_N , as well as by the logarithmic temperature dependence of the resistivity,¹⁰ characteristic of Kondo lattice compounds.

The magnetic ordered state consists of an anisotropic spin density wave, that is incommensurate with the lattice^{9,11} and

opens a gap of the order of 8 K in the Fermi surface, below T_N .¹¹⁻¹³ Nuclear quadrupolar resonance¹¹ and neutron diffraction⁹ experiments indicate that the Ce magnetic moments, antiferromagnetically ordered, lie completely in the basal plane developing a helicoidal structure along the c axis. Specific heat measurements^{12,13} show an abrupt drop of the Sommerfeld coefficient γ below T_N confirming the gapping of the Fermi surface.

The layered structure suggests an important two-dimensional (2D) character supported by the spiral magnetic structure: magnetic order in the planes, weakly coupled between them. However, transport¹⁰ and susceptibility¹⁴ measurements show very little anisotropy. Inelastic neutron scattering,¹⁵ as well, indicates that three-dimensional magnetic fluctuations are relevant. de Haas van Alphen measurements reveal a multiband Fermi surface that might explain the varying role of the anisotropy.¹⁶

The ground state of CeRhIn_5 can also be tuned by chemical substitution. Out-of-plane doping in $\text{CeRh}_{1-y}\text{Ir}_y\text{In}_5$ reveals an interesting coexistence of antiferromagnetism and superconductivity in the range $0.25 < x < 0.60$.¹⁷ In-plane doping in $\text{Ce}_{1-x}\text{La}_x\text{RhIn}_5$ also exhibits interesting features. The incommensurate SDW is seen up to $x \approx 0.4$, where T_N goes to zero.¹⁸ NFL behavior is observed around this critical concentration, perhaps related to the development of an expected quantum critical point.⁷ A “hump” also appears around $T_{\text{SR}} = 4$ K in specific heat and magnetic susceptibility measurements that are claimed to be associated with short-range magnetic correlations,^{7,18,19} as inferred also by NQR and NMR experiments.²⁰

In this work, we present thermal-expansion and magnetostriction results on $\text{Ce}_{0.6}\text{La}_{0.4}\text{RhIn}_5$ single crystals. As in the other free energy second derivatives techniques, namely, specific heat and magnetic susceptibility, the short-range correlations are unambiguously detected by thermal expansion. A large *peak* is observed at $T_{\text{SR}} \sim 4.5$ K but, interestingly, this feature shows up only along the c axis, confirming that the dimensionality plays a relevant role in these 115 compounds. As in the pure compound, crystal electric field (CEF) effects

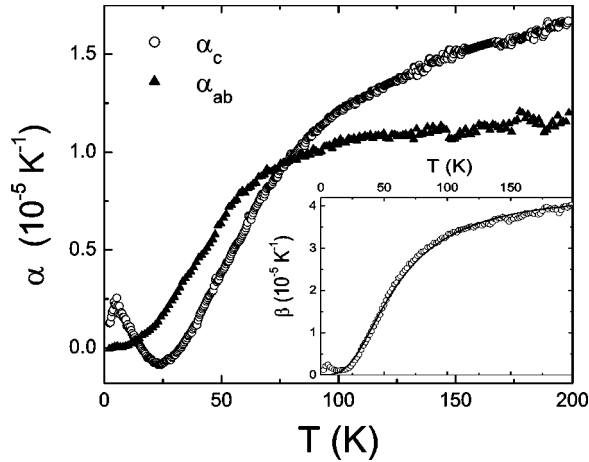


FIG. 1. Linear thermal expansion vs temperature along the c axis (α_c) and perpendicular to it (α_{ab}). Inset: Volume thermal expansion and the estimated lattice contribution ($\Theta_D=245$ K).

are important. The magnetic field dependence of the CEF contribution to the thermal expansion seems to reinforce the idea of a $|\pm 5/2\rangle$ -rich ground state doublet. On the other hand, magnetostriction measurements do not show any particular behavior associated with magnetic correlations. The field dependence of the volume is quadratic in field as expected for a paramagnetic system, above and below T_{SR} .

II. RESULTS

$\text{Ce}_{0.6}\text{La}_{0.4}\text{RhIn}_5$ single crystals were grown by the self-flux technique. For thermal-expansion and magnetostriction measurements we use a $2.6 \times 3.6 \times 7$ mm³ high quality sample [as evidenced by the observation of quantum oscillations up to 30 K (Ref. 21)]. The thermal-expansion experiments were performed using a capacitance dilatometer.

Figure 1 displays the linear thermal-expansion coefficient $\alpha = 1/L(dL/dT)$ along the c axis of the crystal and perpendicularly to it (i.e., along the ab -basal plane), α_c and α_{ab} , respectively. The peak observed at low temperatures in α_c is a magnetic effect while the negative contribution around 25 K is associated with crystal electric field (CEF) effects, as reported by Takeuchi *et al.*¹⁴ in the pure CeRhIn_5 and by Malinowski *et al.*²² in the related Ce_2RhIn_8 .

The volume thermal expansion $\beta = 1/V(dV/dT)$, which for a tetragonal symmetry can be calculated as $\beta = \alpha_c + 2\alpha_{ab}$, is shown in the inset of Fig. 1. Also shown in this inset is the Debye curve corresponding to $\theta_D=245$ K, claimed to be the Debye temperature for the nondoped CeRhIn_5 as inferred from specific heat measurements in the nonmagnetic analog LaRhIn_5 .³ The lattice contribution fits quite well the experimental data above 15 K due to a partial cancellation of the CEF contributions that is negative along the c axis and positive in the basal plane as shown below.

III. DISCUSSION

The deviation of the total thermal expansion from the lattice and the CEF calculated contributions becomes strong

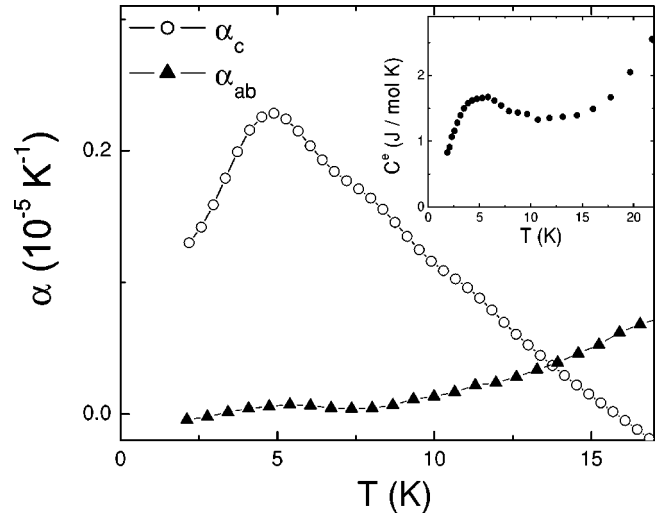


FIG. 2. Low-temperature linear thermal expansion showing the short-range correlations associated peak. Inset: Electronic specific heat vs temperature showing also a feature around 4.5 K (symbols).

below 15 K, as reported also by Takeuchi *et al.*¹⁴ in CeRhIn_5 and Malinowski *et al.*²² in Ce_2RhIn_8 . This temperature marks the onset of the magnetic correlations. Figure 2 shows the low temperature behavior of both α_c and α_{ab} . A peak is observed in α_c at $T_{SR} \sim 4.5$ K, but only a very tiny “bump” is seen in α_{ab} associated with this feature. The antiferromagnetic transition vanishes at $x=0.4$.¹⁸ Thus, this peak may be related to short-range magnetic correlations as was observed in specific heat and susceptibility experiments in $x=0.5$ single crystals.^{7,18,19} The inset of Fig. 2 shows the temperature dependence of the electronic contribution to the specific heat (C^e) for a $x=0.4$ sample, which is quite similar to that reported for $x=0.5$.⁷ The subtracted lattice contribution was inferred from an estimate of the Debye temperature of the nonmagnetic analog LaRhIn_5 . The important conclusion to be drawn from the thermal-expansion data is the anisotropic manifestation of the short-range magnetic correlations, being observed only along the c axis.

This anisotropic behavior is an indication of the anisotropic nature of the interaction between the spins and the lattice, that is, of the spin-orbit coupling. A full understanding of the magnetoelastic tensor would provide a comprehensive explanation of the thermal-expansion results. Although theoretically this is a very difficult enterprise, from magnetostriction experiments we can obtain information about the magnetoelastic tensor in some special directions, as well as further information regarding the magnetic correlations.

Linear magnetostriction data (for fields applied in the basal plane) are shown in Fig. 3 for two different temperatures: one below and the other slightly above T_{SR} , 1.8 and 5 K. The field is applied parallel to the sample dimension being tested. As inferred from the inset, the field dependence of $\Delta L_{ab}/L_{ab}$ is quadratic below and above T_{SR} , as expected for a paramagnetic system.^{22,23} This fact strengthens the conclusion that features observed at T_{SR} in thermal-expansion and specific heat measurements are due to short-range correla-

tions. If long-range order were present, $\Delta L/L$ would have different field dependencies above and below T_{SR} . The temperature dependence of $\Delta L_{ab}/L_{ab}$ is very small in this low-temperature region (in any field configuration). Moreover, the field dependence of $\Delta L_c/L_c$ (not shown here) increases with temperature. This behavior was already reported by Malinowski *et al.*²² in the related Ce_2RhIn_8 , and was ascribed to the magnetic correlations. The same quadratic behavior is observed along the c axis and in any field direction. However, the field dependence of $\Delta L_c/L_c$ (with B along the basal plane) is one order of magnitude larger than the result observed in Fig. 4.

These observations offer a natural explanation for the anisotropic manifestation of the magnetic correlations observed in α . Using a 2D anisotropic Ising model, Light *et al.*⁷ suggested that the disorder introduced by La doping cancels out the interplane magnetic correlations. At $x \sim 0.5$ only short range in-plane correlations remain, and these become evident around T_{SR} . As the Ce magnetic moments lie in the plane, one can naively expect that the local magnetic field associated with these moments is mainly directed in the basal plane. Our magnetostriction results tell us that in this case (field in the plane) the magnetovolume effects are much larger in the c axis than in the plane. Similarly, thermal-expansion measurements in pure $CeRhIn_5$ ¹⁴ reveal that the peak associated with T_N is larger in α_c than in α_{ab} .

Finally, we consider in greater detail the contribution of crystal electric field splitting to thermal expansion. Of particular interest is the extent to which the CEF splitting evolves with x in $Ce_{1-x}La_xRhIn_5$. The Ce^{3+} $J=5/2$ multiplet splits in three doublets in the presence of tetragonal point symmetry:²⁴

$$\Gamma_7^{(2)} = \sqrt{(1-\eta^2)}|\pm 5/2\rangle - \eta|\mp 3/2\rangle,$$

$$\Gamma_7^{(1)} = \eta|\pm 5/2\rangle + \sqrt{(1-\eta^2)}|\mp 3/2\rangle,$$

$$\Gamma_6 = |\pm 1/2\rangle. \quad (1)$$

Neutron scattering results²⁵ on pure $CeRhIn_5$ reveal that $\Gamma_7^{(2)}$ is the ground state doublet, while $\Gamma_7^{(1)}$ at $\Delta_1 = 80$ K and Γ_6 at $\Delta_2 = 274$ K are the first and second excited states, respectively. A value of 0.6 is obtained for the mixing parameter η .

Within the formalism of Morin *et al.*²⁶ that takes into account CEF, quadrupolar and magnetoelastic effects, the contribution to linear thermal-expansion for a tetragonal solid can be estimated as

$$\alpha_c = A \frac{d\langle O_2^0 \rangle}{dT},$$

$$\alpha_{ab} = B \frac{d\langle O_2^0 \rangle}{dT}, \quad (2)$$

where A and B are temperature independent functions of the elastic constants and magnetoelastic coefficients and O_2^0 is the relevant Stevens equivalent operator. The thermodynamic expectation value of this operator $\langle O_2^0 \rangle$ can be calculated through Eq. (1).

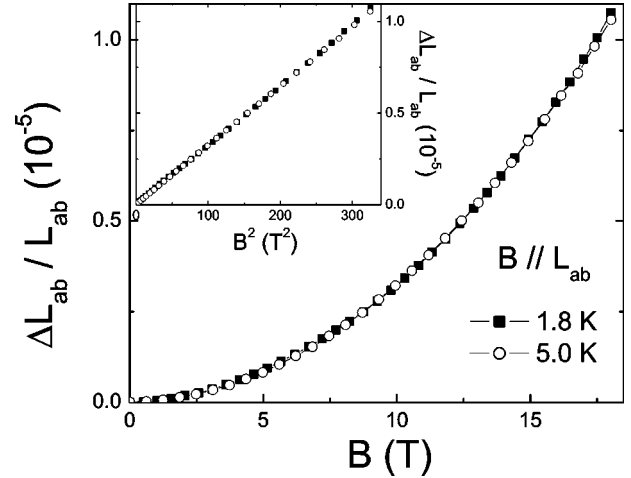


FIG. 3. In-plane linear magnetostriction for fields applied parallel to the dimension that is being tested, at two different temperatures. Inset: magnetostriction as a function of B^2 .

In Fig. 4 we show the electronic linear thermal-expansion along the c axis (α_c^e , upper panel) and perpendicular to it (α_{ab}^e , lower panel) after subtracting the lattice contribution, estimated from the $\theta_D = 245$ K Debye curve. The solid lines are the CEF contributions derived from Eq. (2), using the values for η , Δ_1 , and Δ_2 obtained from neutron scattering experiments in the pure compound.²⁵ The only free parameters are the T -independent coefficients A and B , that are set such that the maxima coincide. The detailed agreement is rather poor, especially for α_c^e , although the overall shape is correct.

In Fig. 5 we show α_c as a function of temperature for different magnetic fields applied along the c axis. Experimentally, the minimum in α_c associated with CEF effects

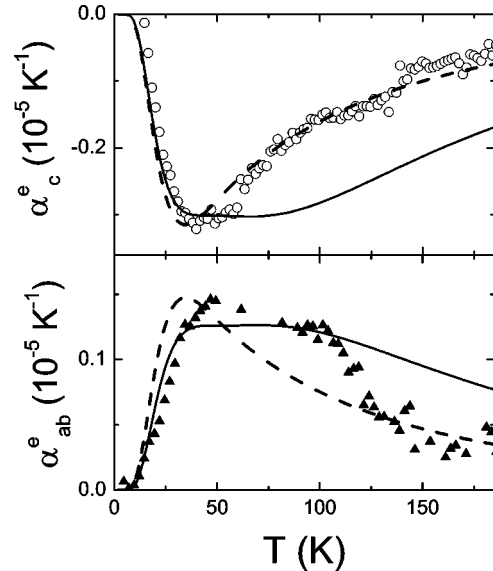


FIG. 4. Electronic contribution to the thermal expansion (symbols). Solid line: CEF fit using parameters from neutron scattering measurements (see text). Dashed line: *idem* but with mixing parameter $\eta=0$. Upper panel: α_c . Lower panel: α_{ab} .

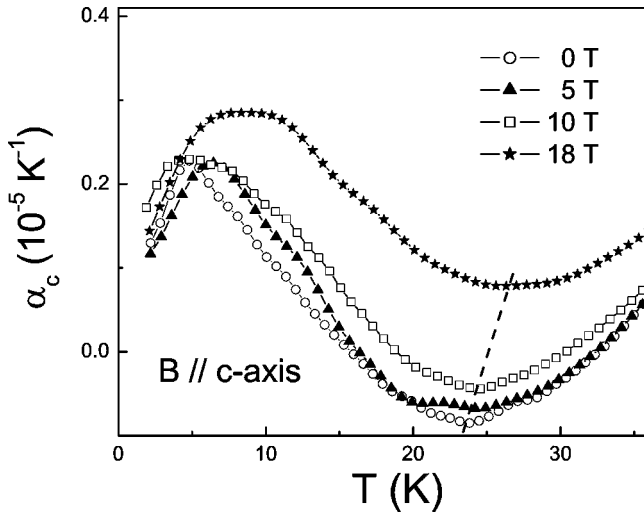


FIG. 5. Linear thermal-expansion α_c for different magnetic fields applied along the c axis.

clearly shifts to higher T with increasing field. The magnetic field splits the three doublets and, according to our CEF scheme, mixes together $\Gamma_7^{(2)}$ and $\Gamma_7^{(1)}$. So, the full diagonalization of the complete Hamiltonian (CEF plus Zeeman) results in six singlet states. An estimate of α_c^{CEF} (18 T) according to this new scheme can be observed in the upper panel of Fig. 6. In the same figure $\alpha_c^{\text{CEF}}(0)$ is shown for comparison. In our calculation the absolute value of the c axis thermal expansion has a large increase and the minimum moves down from $T \sim 42$ to 12 K when applying 18 T (parallel to the c axis). This huge change comes from the Zeeman splitting (~ 40 K for $B = 18$ T) of the ground state doublet that must be compared with the original $\Delta_1 = 80$ K separation to the first excited state in zero field. As a result, the first excited state starts to be populated at much lower T when a field is applied and, thus, the associated peak occurs at lower T as well. This predicted behavior is in direct contradiction with what we observe experimentally.

According to Eq. (2), there would be no maxima in thermal expansion associated with the population of the first excited singlet if the expectation value of O_2^0 is the same in both the ground and the first excited singlet. This occurs when the mixing parameter η vanishes. The lower panel of Fig. 6 shows the calculated $\alpha_c^{\text{CEF}}(0)$ and $\alpha_c^{\text{CEF}}(18 \text{ T})$ for $\eta = 0$. The absolute value of the minimum slightly decreases and moves weakly toward higher T . This behavior is much more consistent with our experimental observation. In the case that $\eta = 0$, the ground state doublet $\Gamma_7^{(2)}$ is now a pure $|\pm 5/2\rangle$ state while the first excited $\Gamma_7^{(1)}$ is a pure $|\pm 3/2\rangle$. Using this approach, we estimate the temperature dependent thermal expansion. This result is shown as the dashed curves in Fig. 4 using the same Δ_1 and Δ_2 as for the solid lines. At least along the c axis, the agreement with the experimental results is much better. On the other hand, if $\eta = 0$ in undoped

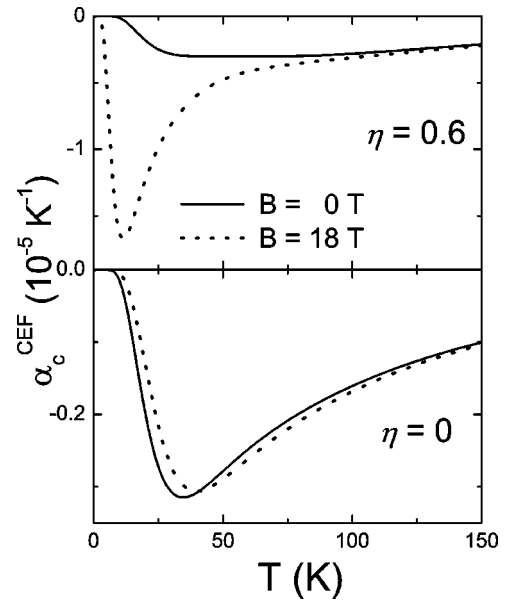


FIG. 6. Calculation of the CEF contribution to the c axis thermal expansion for zero field and 18 T. Upper panel: using a mixing parameter $\eta = 0.6$. Lower panel: $\eta = 0$.

CeRhIn₅, then the peak observed in inelastic neutron scattering experiments²⁵ at 23 meV would be forbidden by symmetry. Thus, from these observations we hypothesize that substituting La for Ce leads to a decrease in the mixing parameter η , due presumably to chemical pressure effects and changes in hybridization strength. However, La doping seems to have no major effect on the level splitting.

IV. CONCLUSIONS

Thermal expansion measurements were performed in Ce_{0.6}La_{0.4}RhIn₅ single crystals. Short-range magnetic correlations are clearly detected as a “hump” at $T_{\text{SR}} \sim 4.5$ K, as observed also in specific heat and magnetic susceptibility experiments. This feature is observed only along the c axis confirming the anisotropic nature of this compound. As expected for a paramagnetic system, magnetostriction experiments show a quadratic field dependence of the volume above and below T_{SR} indicating that this magnetic-related anomaly cannot be associated with a long-range order. Finally, La doping appears to increase the $|\pm 5/2\rangle$ character of the crystal electric field ground state doublet in Ce_{1-x}La_xRhIn₅.

ACKNOWLEDGMENT

We gratefully acknowledge C. D. Batista for helpful discussions and F. Drymiotis for his collaboration in the specific heat experiments. Work at the NHMFL was performed under the auspices of the National Science Foundation, the State of Florida, and the U.S. Department of Energy.

- ¹See, for example, the review N. Grewe and F. Steglich, in *Handbook on the Physics and Chemistry of Rare Earths*, edited by K. A. Gschneidner, Jr. and L. Eyring (Elsevier Science Publishers, Amsterdam, 1991), Vol. 14, p. 343.
- ²A.C. Hewson, in *The Kondo Problem to Heavy Fermions*, edited by D. Edwards and D. Melville (Cambridge University Press, United Kingdom, 1992).
- ³H. Hegger, C. Petrovic, E.G. Moshopoulou, M.F. Hundley, J.L. Sarrao, Z. Fisk, and J.D. Thompson, *Phys. Rev. Lett.* **84**, 4986 (2000).
- ⁴C. Petrovic, R. Movshovich, M. Jaime, P.G. Pagliuso, M.F. Hundley, J.L. Sarrao, Z. Fisk, and J.D. Thompson, *Europhys. Lett.* **53**, 354 (2001).
- ⁵C. Petrovic, P.G. Pagliuso, M.F. Hundley, R. Movshovich, J.L. Sarrao, J.D. Thompson, Z. Fisk, and P. Monthoux, *J. Phys.: Condens. Matter* **13**, L337 (2001).
- ⁶V.S. Zapf, N.A. Frederick, K.L. Rogers, K.D. Hof, P.C. Ho, E.D. Bauer, and M.B. Maple, *Phys. Rev. B* **67**, 064405 (2003).
- ⁷B.E. Light, Ravhi S. Kumar, A.L. Cornelius, P.G. Pagliuso, and J.L. Sarrao, *Phys. Rev. B* **69**, 024419 (2004).
- ⁸R.A. Fisher, F. Bouquet, N.E. Phillips, M.F. Hundley, P.G. Pagliuso, J.L. Sarrao, Z. Fisk, and J.D. Thompson, *Phys. Rev. B* **65**, 224509 (2002).
- ⁹W. Bao, P.G. Pagliuso, J.L. Sarrao, J.D. Thompson, Z. Fisk, J.W. Lynn, and R.W. Erwin, *Phys. Rev. B* **62**, 14621 (2000); **63**, 219901(E) (2001); **67**, 099903(E) (2003).
- ¹⁰A.D. Christianson, A.H. Lacerda, M.F. Hundley, P.G. Pagliuso, and J.L. Sarrao, *Phys. Rev. B* **66**, 054410 (2002).
- ¹¹N.J. Curro, P.C. Hammel, P.G. Pagliuso, J.L. Sarrao, J.D. Thompson, and Z. Fisk, *Phys. Rev. B* **62**, 6100 (2000).
- ¹²A.L. Cornelius, A.J. Arko, J.L. Sarrao, M.F. Hundley, and Z. Fisk, *Phys. Rev. B* **62**, 14 181 (2000).
- ¹³A.L. Cornelius, P.G. Pagliuso, M.F. Hundley, and J.L. Sarrao, *Phys. Rev. B* **64**, 144411 (2001).
- ¹⁴T. Takeuchi, T. Inoue, K. Sugiyama, D. Aoki, Y. Tokiwa, Y. Haga, K. Kindo, and Y. Onuki, *J. Phys. Soc. Jpn.* **70**, 877 (001).
- ¹⁵W. Bao, G. Aeppli, J.W. Lynn, P.G. Pagliuso, J.L. Sarrao, M.F. Hundley, J.D. Thompson, and Z. Fisk, *Phys. Rev. B* **65**, 100505 (2002).
- ¹⁶D. Hall, E.C. Palm, T.P. Murphy, S.W. Tozer, C. Petrovic, E. Miller-Ricci, L. Peabody, C.Q.H. Li, U. Alver, R.G. Goodrich, J.L. Sarrao, P.G. Pagliuso, J.M. Wills, and Z. Fisk, *Phys. Rev. B* **64**, 064506 (2001).
- ¹⁷P.G. Pagliuso, C. Petrovic, R. Movshovich, D. Hall, M.F. Hundley, J.L. Sarrao, J.D. Thompson, and Z. Fisk, *Phys. Rev. B* **64**, 100503 (2001).
- ¹⁸P.G. Pagliuso, N.O. Moreno, N.J. Curro, J.D. Thompson, M.F. Hundley, J.L. Sarrao, Z. Fisk, A.D. Christianson, A.H. Lacerda, B.E. Light, and A.L. Cornelius, *Phys. Rev. B* **66**, 054433 (2002).
- ¹⁹J.S. Kim, J. Alwood, D. Mixson, P. Watts, and G.R. Stewart, *Phys. Rev. B* **66**, 134418 (2002).
- ²⁰Y. Iwamoto, K. Ueda, T. Kohara, Y. Kohori, V.S. Zapf, T.A. Sayles, M.B. Maple, and J.L. Sarrao (unpublished).
- ²¹V.F. Correa *et al.* (unpublished).
- ²²A. Malinowski, M.F. Hundley, N.O. Moreno, P.G. Pagliuso, J.L. Sarrao, and J.D. Thompson, *Phys. Rev. B* **68**, 184419 (2003).
- ²³J. Ziegłowski, H.U. Häfner, and D. Wohlleben, *Phys. Rev. Lett.* **56**, 193 (1986).
- ²⁴T. Ohama, H. Yasuoka, D. Mandrus, Z. Fisk, and J.L. Smith, *J. Phys. Soc. Jpn.* **64**, 2628 (1995).
- ²⁵A.D. Christianson, J.M. Lawrence, P.G. Pagliuso, N.O. Moreno, J.L. Sarrao, J.D. Thompson, P.S. Riseborough, S. Kern, E.A. Goremychkin, and A.H. Lacerda, *Phys. Rev. B* **66**, 193102 (2002).
- ²⁶P. Morin, J. Rouchy, and D. Schmitt, *Phys. Rev. B* **37**, 5401 (1988).